

Supplementary Information

S1 Distributions of residence time and extinction event sizes

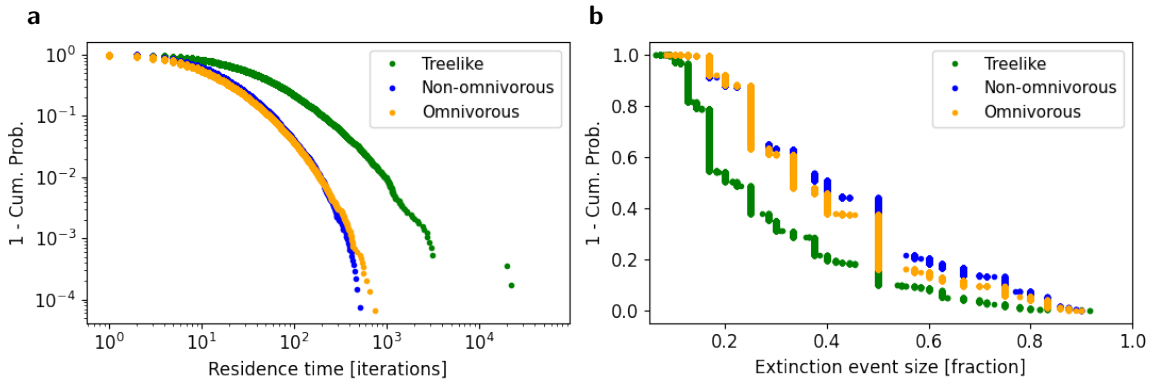


Figure S1: **Vulnerability of resident species in three types of food webs.** **a**, Cumulative probability distribution of residence times. **b**, Cumulative probability distribution of extinction event size.

Resident times (Fig. S1a) and fractional extinction event sizes (Fig. S1b) of three different food web types. Resident times in all three food webs fall off approximately like $\propto \exp(-bt^{1/c})$, though this function gets less accurate for larger t . For the treelike food web we observe $b \approx 11$ and $c \approx 9$, whereas for the two food webs with network loops we observe $b \approx 12.5$ and $c \approx 8$.

S2 Example of extinction cascade

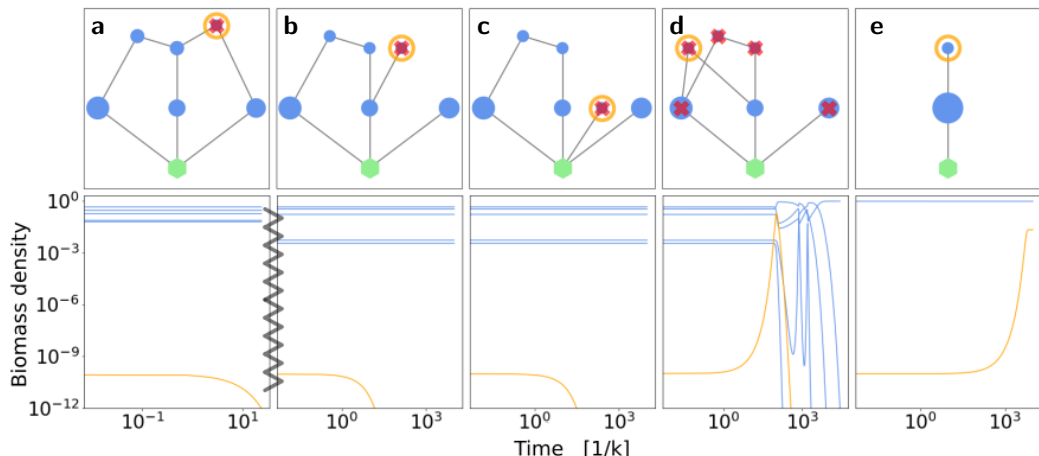


Figure S2: **Example of extinction cascade.** **a–e**, Five invasion attempts in an omnivorous food web with $\beta = 0.75$. Presentation and labelling analogous to that in Fig. 2. The figures correspond to the invasion attempts 76901, 76913–76916. **a**, Unsuccessful invasion attempt by omnivorous invader; **b**, Unsuccessful invasion attempt by consumer of one resource; **c**, Unsuccessful invasion attempt by primary producer; **d**, The invader causes an extinction cascade killing itself along with four resident species; **e**, Successful invasion by a species consuming the only resident species in the food web.

S3 Analytical spectrum of food webs with two species

The only feasible food web with two species is that of one producer and one species consuming the producer. The steady states of this food web are

$$S_1^* = \frac{\alpha_2}{\beta\eta}, \quad S_2^* = \frac{k}{\eta} \left(1 - \frac{\alpha_2}{\beta\eta} \right) - \frac{\alpha_1}{\eta} \quad (\text{S1})$$

for the producer and consumer, respectively. Here $\beta = \beta_{21}$ and $\eta = \eta_{21}$. Inserting this in eq. (5) and diagonalising yields the eigenvalues

$$\lambda_{\pm} = -\frac{k\alpha_2}{2\beta\eta} \pm \sqrt{\left(\frac{k\alpha_2}{2\beta\eta}\right)^2 + \frac{k\alpha_2^2}{\beta\eta} - (k - \alpha_1)\alpha_2}. \quad (\text{S2})$$

The food web is stable if the real parts of all eigenvalues are negative. The real part of $\text{Re}(\lambda_-)$ is always negative. $\text{Re}(\lambda_+)$ is only *non-negative* if the square root is real and equal to or greater than $\frac{k\alpha_2}{2\beta\eta}$. After some basic algebraic operations this criterion reduces to the following restriction on the species parameters

$$1 < \frac{\alpha_1}{k} + \frac{\alpha_2}{\beta\eta}. \quad (\text{S3})$$

Eq. (S3) is further restricted by feasibility of the food web, which requires the steady states of eq. (S1) to be positive. S_1^* is always positive, but S_2^* is only positive if $\beta\eta > \frac{\alpha_2}{1-\alpha_1/k}$. Inserting this in eq. (S3) now yields

$$1 < \frac{\alpha_1}{k} + \frac{\alpha_2}{\beta\eta} < \frac{\alpha_1}{k} + \frac{\alpha_2}{\alpha_2} \left(1 - \frac{\alpha_1}{k} \right) = 1. \quad (\text{S4})$$

This condition can never be satisfied and consequently a feasible food web with two species will always be stable.

The eigenvalues are purely real if the square root of eq. (S3) is bigger than or equal to zero. Again using some basic algebra this criterion transforms to

$$(\beta\eta)^2 - \gamma\beta\eta - 0.25\gamma k \leq 0, \quad \text{with } \gamma \equiv \frac{\alpha_2}{1 - \alpha_1/k}. \quad (\text{S5})$$

This second order polynomial is zero when

$$(\beta\eta)_{\pm} = \frac{1}{2} \left(\gamma \pm \sqrt{\gamma^2 + k\gamma} \right), \quad (\text{S6})$$

and negative in the interval between the two roots. $(\beta\eta)_-$ is always negative, since $k\gamma > 0$ for all $\alpha_1 < k$. This root is not physically meaningful. Accordingly, the eigenvalues are purely real if and only if $\beta\eta \leq (\beta\eta)_+$.

S4 Omnivorous eigenvalue spectra of species richness 2–10

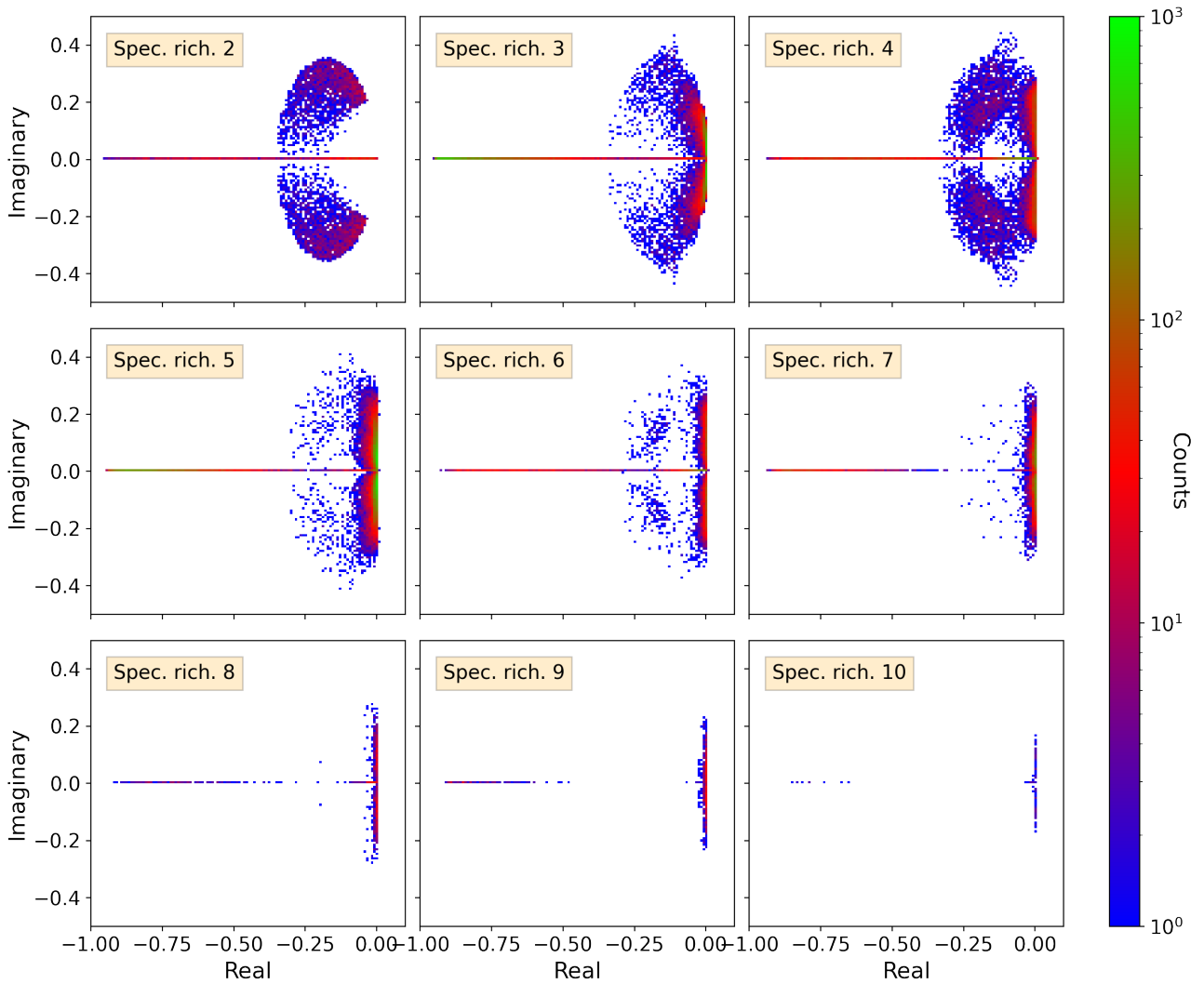


Figure S3: Complex eigenvalue spectra of evolved omnivorous food webs with $\beta = 0.75$. Each panel represents the two-dimensional histogram in the complex plane. Species richness as labelled in panels. Note that the colour scale is logarithmic, with green marking the areas with largest likelihood of eigenvalues. Left row corresponds to the omnivorous food webs in Fig. 3. As discussed in the main text, changing the invasion mechanics does not affect the spectrum notably.

S5 Average connectivity of the community matrix

Type	Frequency in food web, f	Interaction links, L
Producers	$(N+2)/3N$	$(N+2)(N-1)/3N$
Consumer of 1	$N/3N$	$1 \cdot 2$
Consumer of 2	$(N-2)/3N$	$2 \cdot 2$

Table S2: Frequencies and number of off-diagonal entries of the three types of species in a omnivorous food web of species richness $N > 1$, as used for computing the occupation probability in the random matrices in Fig. 4.

The connectivity of the community matrix is equal to the number of interaction links in the food web, divided by the total number of elements in the matrix, multiplied by two, since every interaction appears twice in the community matrix. Here, we disregard the diagonal of the community matrix since it represents self regulation and is therefore always present in the community matrix. There are three types of species in an omnivorous food web, in terms of number of interaction links: *primary producers*, with links to all other primary producers, *consumers with one resource*, and *consumers with two resources*. In addition, any of the three can also be the resource of another species.

In Tab. S2 we list the occurrence frequency of each species type in a food web of species richness $N > 1$, assuming no extinctions occur. The probability that an invasive species is a primary producer is $1/3$. Furthermore, all food webs are initialised with a primary producer. The average number of primary producers is therefore $1+(N-1)/3 = (N+2)/3$. The probability that an invasive consumer has only one resource is 1 for $N = 2$, and $1/2$ for $N > 2$. The average number of consumers of a single resource is therefore $\frac{2}{3} + \frac{2}{3} \cdot \frac{1}{2}(N-2) = N/3$, whereas the average number of consumers with two resources is $\frac{2}{3} \cdot \frac{1}{2}(N-2) = (N-2)/3$.

In the second column we list the number of interaction links that each species type adds to the community matrix. Primary producers have interaction links to all other primary producers, i.e. on average every primary producer has $L_{prod} = (N-1) \cdot f_{prod}$ interaction links. Consumers have 1 or 2 interaction links, depending on their number of resources. Since every consumer-resource interaction also appears in the row of the resource species, we multiply the number of consumer interaction links by 2. The total number of non-zero off-diagonal elements in the community matrix now becomes

$$N \sum_{type} L_{type} \cdot f_{type} = (N-1)f_{prod}f_{prod} + 2Nf_{cons_1} + 4Nf_{cons_2}. \quad (\text{S7})$$

Dividing this by the total number of off-diagonal entries, $N(N-1)$, we obtain the probability that an entry in the community matrix is non-zero

$$\begin{aligned} p &= \frac{N+2}{3N} \cdot \frac{(N+2)(N-1)}{3N(N-1)} + 2\frac{N}{3N} \cdot \frac{1}{N-1} + 4\frac{N-2}{3N} \cdot \frac{2}{N-1}, \\ \Rightarrow p &= \frac{N^3 + 21N^2 - 24N - 4}{9N(N-1)}. \end{aligned}$$

S6 The effect of β on eigenvalue spectra

Fig. 5 depicts the distributions of eigenvalues along the real axis for different values of β . Here we therefore investigate how the choice of β affects the eigenvalue spectrum. In Fig. S4 histograms of eigenvalues along the real axis are

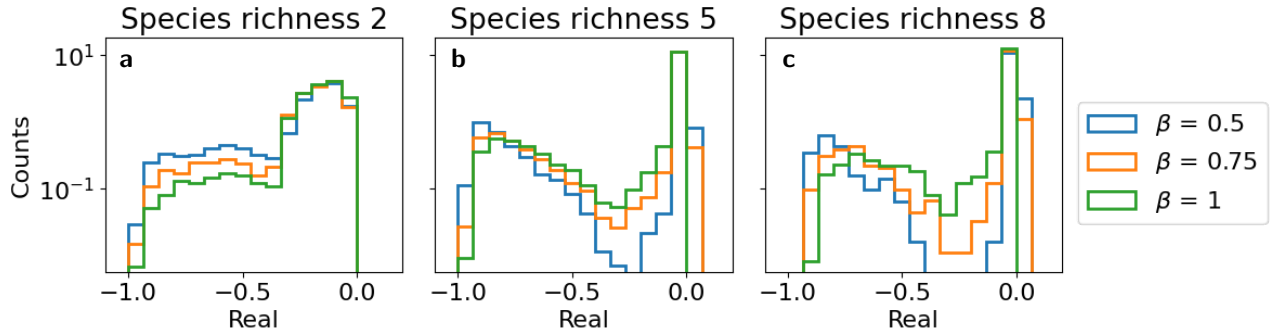


Figure S4: **Histograms of eigenvalues along the real axis for different β .** Normalised frequency histograms of eigenvalues along the real axis for omnivorous food webs.

plotted for $\beta = 0.5, 0.75$ and 1 . The range and overall shape are similar. For species richness 2 (Fig. S4a) the left plateau decreases in significance with increasing β . For larger species richness (Fig. S4b and c) the middle region is less depleted for high β , i.e. the spectra become "less" biomodal with β . Even though varying β does affect the distribution of eigenvalues along the real axis, we still combine the distributions in Fig. 5 because they have peaks and dips in the same ranges of real values, and we are interested in comparing the overall shapes of the eigenvalue spectra, rather than the exact distributions.

Fig. S5 shows the corresponding histograms of eigenvalues along the imaginary axis. For all β and species richesses

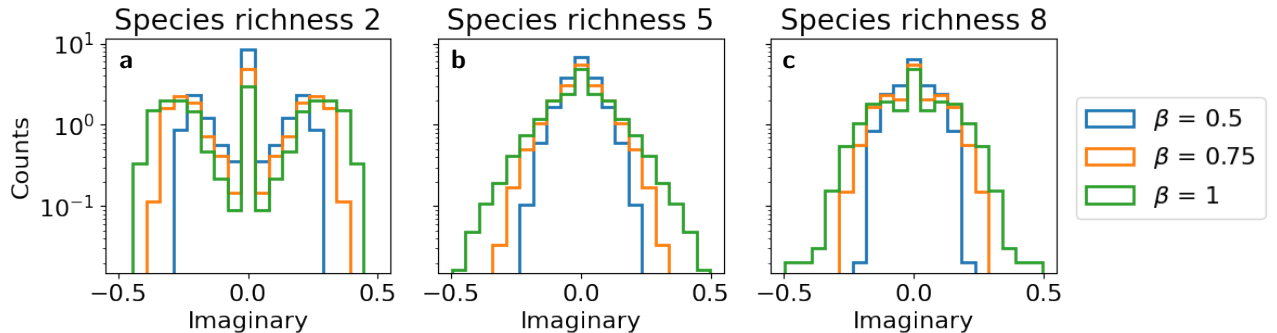


Figure S5: **Histograms of eigenvalues along the imaginary axis for different β .** Normalised frequency histograms of eigenvalues along the imaginary axis for omnivorous food webs.

there is a peak around 0 on the imaginary axis, as expected since most spectra contain a significant fraction of purely real eigenvalues. As β increases, so does the width of the imaginary distribution, whereas the overall shape remains the same.

S7 Class diagrams

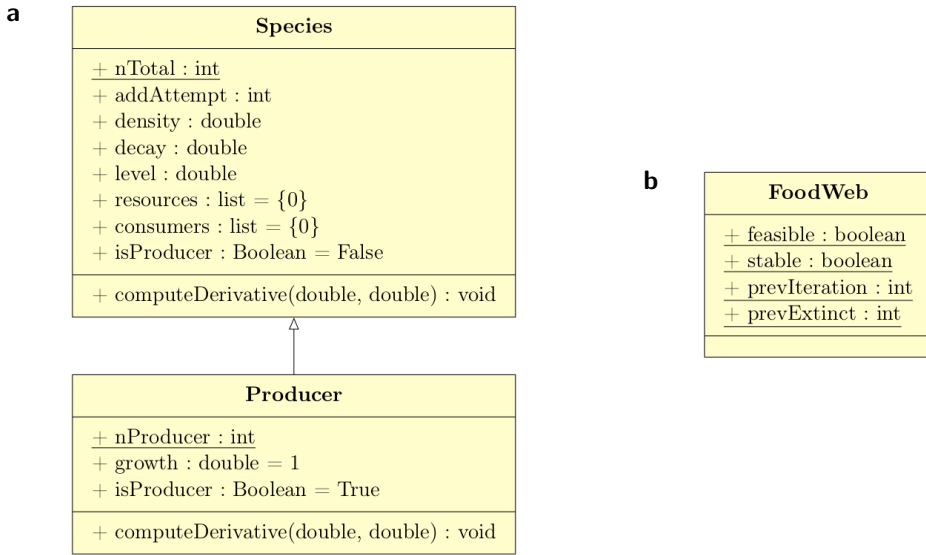


Figure S6: **Class diagrams from simulations.** **a**, the class Species and the derived class Producer. **b** the class FoodWeb.

Fig. S6a depicts the class diagrams of the class Species and the derived class Producer. nTotal is a global variable that keeps track of the total number of species in the food web. addAttempt is the iteration during which a given species invaded the food web. density, decay and level represent S_i , α_i and l_i , respectively. resources and consumers contain interaction parameters to the species' resources and consumers, respectively. That is, resources contains $\beta_{i1}\eta_{i1}, \beta_{i2}\eta_{i2}, \dots, \beta_{in}\eta_{in}$, and consumers contains $\eta_{1i}, \eta_{2i}, \dots, \eta_{ni}$. All η_{ij} and η_{ji} representing interactions that are not present in the food web are set to zero. isProducer is a Boolean variable that is true if the given species is a primary producer and false otherwise. Lastly, the class Species contains the function computeDerivative() that computes the derivative of the given species according to eq. 2.

The class Producer contains the additional global variable nProducer which is the total number of primary producers in the food web. Furthermore, growth represents k_i and computeDerivative() computes the derivative according to eq. 1.

The class FoodWeb is shown in fig. S6b which is mainly created to keep track of indices during the integration. feasible and stable are true if the food web during a given invasion is feasible or linearly stable, respectively, and false otherwise. prevIteration is an integer that describes how the food web behaved after the previous invasion, and is used to optimise detection of non-convergent food webs. If the food web converged to the steady state after the previous invasion, prevIteration is set to one. If the food web did not reach the steady states within the time limit, prevIteration is set to two (linearly stable food webs) or nine (unstable food webs). Finally, prevExtinction represents the previous species to go extinct.

S8 Varying the sampling distributions of α and η

In the main text we draw decay and interaction rates from uniform distributions (see Tab. 1). Here, we run the simulation for omnivorous food webs, drawing α and η from Gaussian and exponential distributions, respectively. The

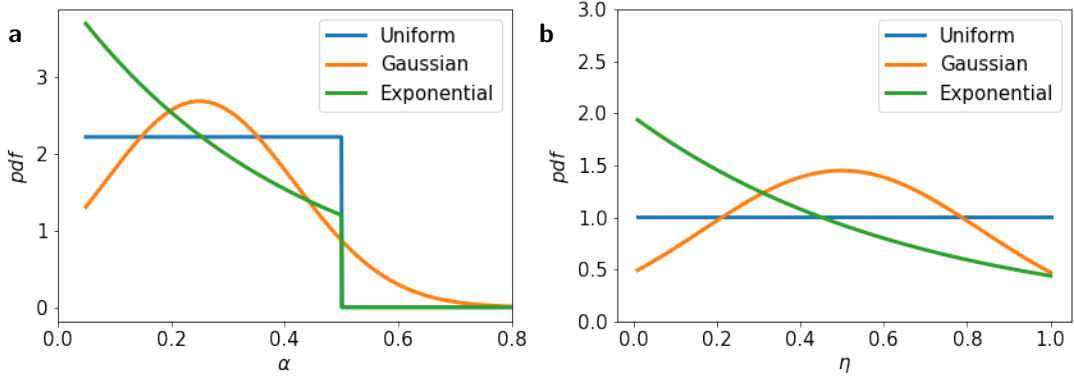


Figure S7: Sampling distributions of α and η . **a**, Sampling distributions of α . Gaussian distribution with $\mu = 0.25$ and $\sigma = 1/6$, exponential distribution with $\lambda = 2.5$. **b**, Sampling distributions of η . Gaussian distribution with $\mu = 0.5$ and $\sigma = 1/3$, exponential distribution with $\lambda = 1.5$.

sample distributions are illustrated in Fig. S7. To avoid unphysical parameter values, a lower bound of 0.05 and 0.01 is imposed on the distributions of α and η , respectively. The η -distributions also have an upper bound of 1, whereas only the exponential α -distribution has an upper bound of 0.5. These bounds are the same as in the uniform case in Tab. 1. Fig. S8 show the resulting distributions of eigenvalues along the real axis for the three different sampling

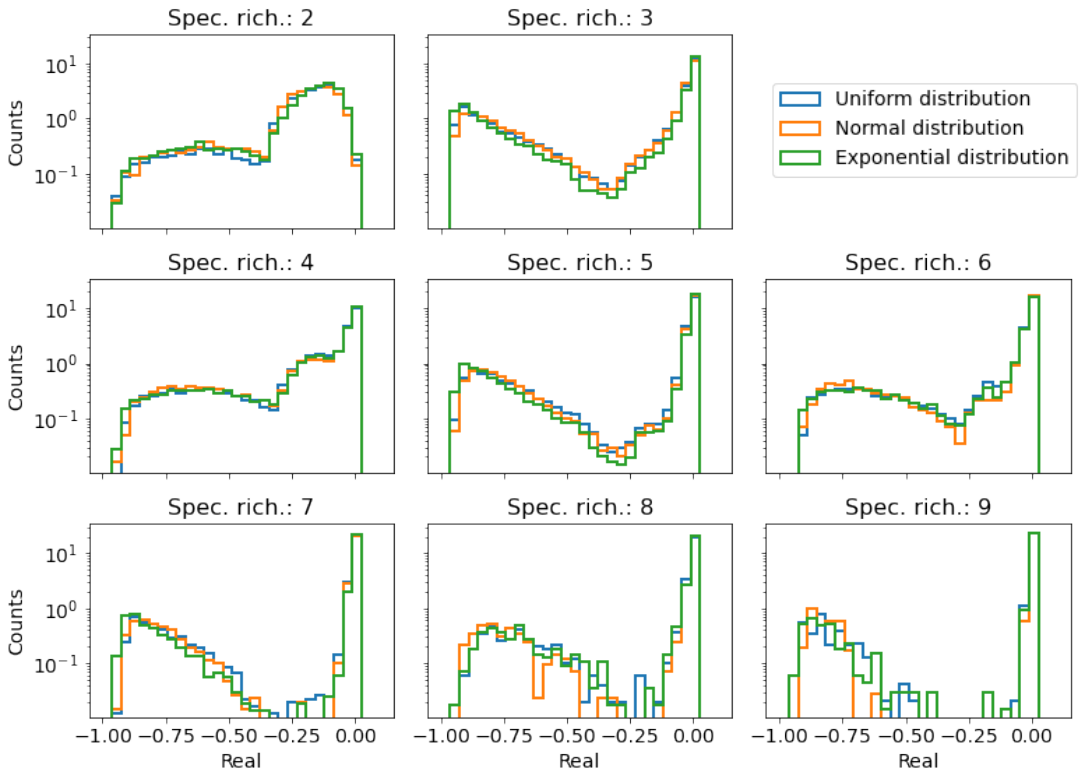


Figure S8: Histograms of eigenvalues along the real axis for different sampling distributions of η and α . The histograms are normalised frequency histograms of eigenvalues along the real axis for omnivorous food webs with species richness 2–9.

distributions of α and η . The eigenvalue distributions are practically identical, thus confirming that our results are robust to small changes in the distributions of parameters.

S9 Holling type-II response

The simulation is extended to allow consumption rates following Holling type-II functional response [47]

$$r(\eta_{ki}, S_i) = \frac{\eta_{ki} S_i}{1 + h\eta_{ki} S_i}, \quad (\text{S8})$$

where S_i is the density of the resource species and η_{ki} is the link specific interaction strength between the resource i and consumer k as defined in Results and Discussion. The parameter h controls the significance of the type-II response. When $h = 0$ Eq. S8 reduces to type-I functional response as used in Eqs. 1–2.

With consumption rates following Holling type-II functional response, the system of equations analogous to Eqs. 1–2 is no longer linear in S . Eq. 4 is therefore not applicable and neither are the convergence criteria described in Materials and Methods. A simpler algorithm is therefore employed in order to compute the eigenvalue spectra here. The food web is now considered to be converged if

$$\left| \frac{\dot{S}_i}{S_i} \right| \leq 10^{-10} \quad \forall i, \quad (\text{S9})$$

and the densities that satisfy Eq. S9 are plugged in as $\mathbf{S}(t)$ in Eq. 5. The overall procedure is shown in Algorithm 2.

Algorithm 2: Pseudo-code of the evolutionary algorithm with type-II functional response

1 initialize food web;

2 **for** each invasion **do**

3 add new species;

4 **while** not converged **do**

5 integrate food web;

6 update time;

7 **if** extinction event **then**

8 remove species;

9 restart time;

10 **end**

11 **if** time $\geq 10^5$ **then**

12 break;

13 **end**

14 **end**

15 compute eigenvalues;

16 **end**

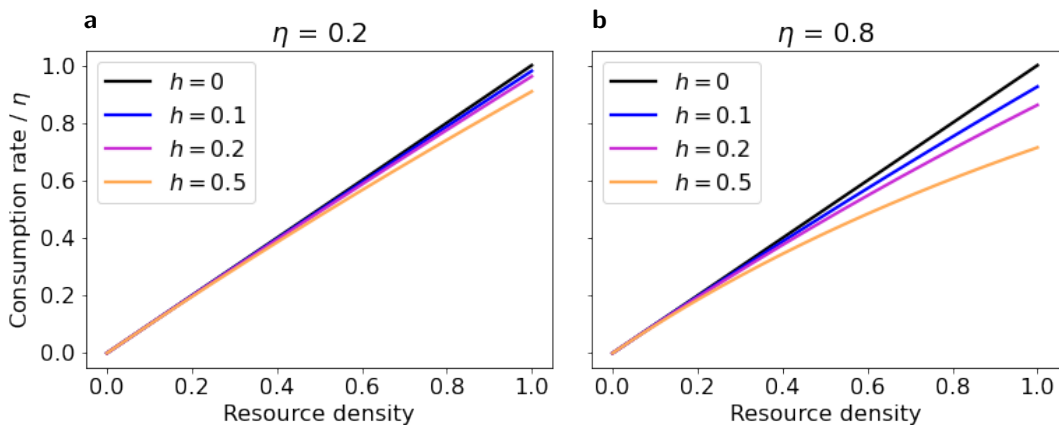


Figure S9: **Consumption rates for different values of h for $\eta = 0.2$ and $\eta = 0.8$.** **a**, $\eta = 0.2$ and the consumption rate changes little with h . **b**, $\eta = 0.8$ and the non-linearity of the consumption rate is more pronounced.

Since the type-II response community matrix eigenvalues are computed only from the food webs that satisfy eq. S9, we only obtain the stable eigenvalues. Starting from $h = 0$, we run the simulation for $h = 0.1, 0.2$ and 0.5 . The effect on the consumption rate can be seen in Fig. S9 for two values of η . In interactions of low interaction strength the non-linear effects are negligible for most h , whereas for high interaction strengths the non-linearity is pronounced

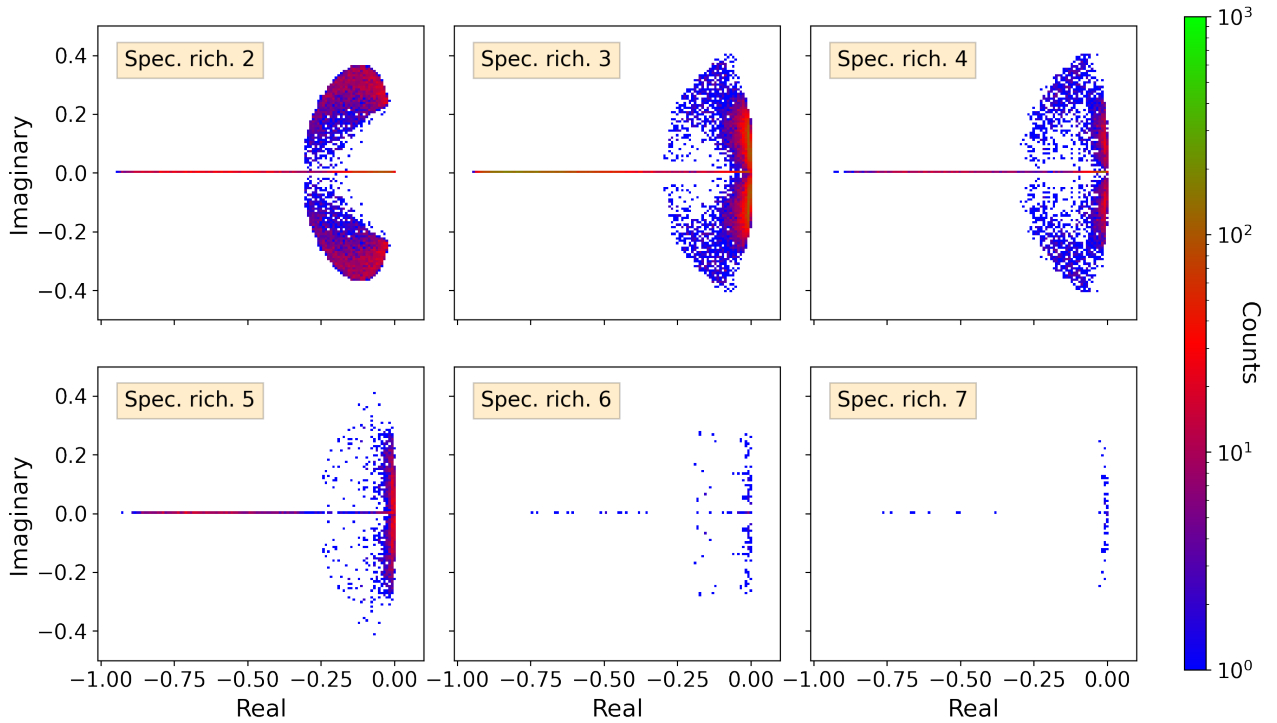


Figure S10: **Complex eigenvalues spectra of evolved omnivorous type-II response food webs with $h = 0.5$.** Each panel represents the two-dimensional histogram in the complex plane. Species richness as labelled in panels and $\beta = 0.75$.

for all h . As we increase h the average species richness decreases, and for $h = 0.5$ there are no convergent food webs of species richness higher than 7, though there are non-convergent food webs of up to 9 species. Fig. S10 shows the stable part of eigenspectra of food webs with species richness 2–7. The type-II spectra resemble the type-I spectra from Fig. S3, but are more skewed towards positive real values. It seems intuitive that interactions following type-II response would act as a dampening, thereby stabilising the food webs and allowing for food webs of higher species richness. To get some insight in why this is seemingly not the case, we study the spectrum of a food web with two species, analogous to S3. The steady states of this food web are

$$S_1^* = \frac{\alpha_2}{\eta\beta'}, \quad S_2^* = \left[\frac{k}{\eta} \left(1 - \frac{\alpha_2}{\eta\beta'} \right) - \alpha_1 \right] \frac{\beta}{\beta'}, \quad \text{with } \beta' \equiv \beta - h\alpha_2, \quad (\text{S10})$$

i.e. similar to the steady states of type-I response, with β' replacing β . From these we see that feasibility now requires

$$1. \quad \beta > h\alpha_2, \quad (\text{S11})$$

$$2. \quad \eta > \frac{1}{\beta'} \frac{\alpha_2}{1 - \alpha_1/k}. \quad (\text{S12})$$

Since $\beta' \leq \beta$ for all h and α_2 , we see that it requires a higher η to satisfy the feasibility criterion of Eq. S12, compared that of type-I response.

Then we study the stability of this food web. First we compute the community matrix according to eq. 5

$$C_{11} = \left(k \left(1 - \frac{\alpha_2}{\beta'\eta} \right) - \alpha_1 \right) \left(1 - \frac{\beta'}{\beta} \right) - \frac{k\alpha_2}{\beta'\eta}, \quad (\text{S13})$$

$$C_{12} = -\frac{\alpha_2}{\beta} < 0, \quad (\text{S14})$$

$$C_{21} = k\beta' \left(1 - \frac{\alpha_2}{\eta\beta'} \right) - \alpha_1\beta' > 0 \quad (\text{from feasibility}), \quad (\text{S15})$$

$$C_{22} = 0. \quad (\text{S16})$$

Since $C_{22} = 0$ and $C_{12}C_{21} < 0$, the quadratic formula for the eigenvalues reduces to

$$2\lambda_{\pm} = C_{11} \pm \sqrt{C_{11}^2 - 4|C_{12}C_{21}|}, \quad (\text{S17})$$

and we see that both eigenvalues are always stable when $C_{11} < 0$, because the square root is always smaller or equal to C_{11} . After some algebra we find the following criterion for stability

$$\eta < \frac{k/h}{k - \alpha_1} \frac{\beta + h\alpha_2}{\beta - h\alpha_2}. \quad (\text{S18})$$

The RHS is always larger than 1 (for $h \leq 1$), which is the upper limit on η . Food webs of species richness 2 are therefore also stable when we introduce Holling type-II response, given that $h \leq 1$. However, they might be unstable for $h > 1$.

We only use $h < 1$ in our simulations, and Eq. S18 is always satisfied with our choice of parameters. Yet the upper limit on η decreases with h , meaning the system somehow becomes "less stable" with h . It therefore seems reasonable that larger food webs with type-II response can indeed be less stable than their type-I counterparts.

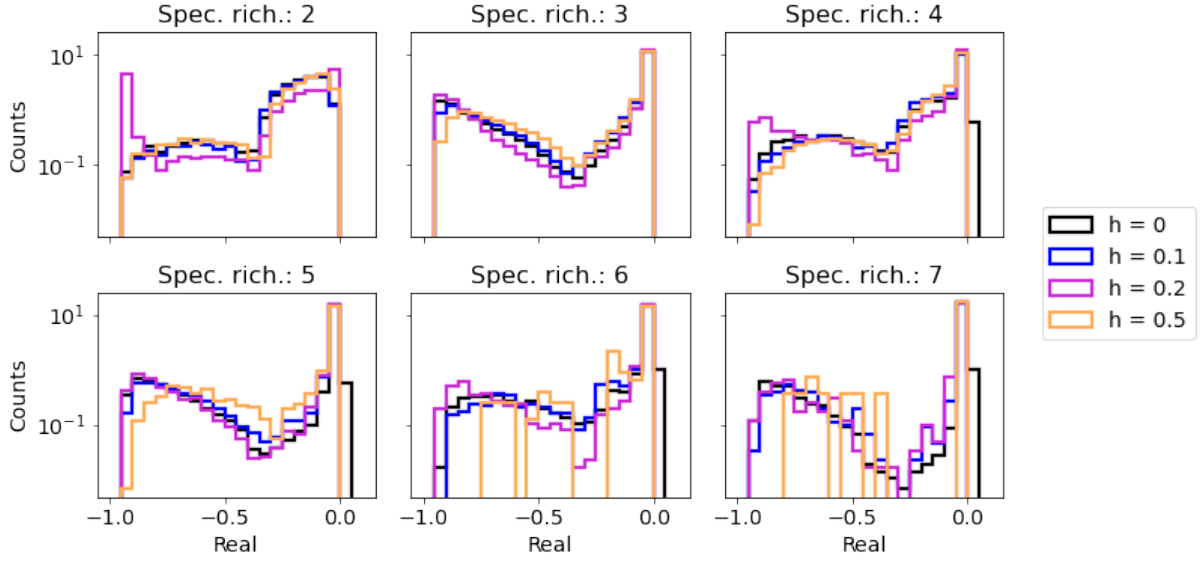


Figure S11: **Distribution of eigenvalues along the real axis**

Lastly, we plot the distributions of type-II eigenvalues along the real axis in Fig. S11. Despite a low number of eigenvalues from the simulation with $h = 0.5$, all distributions appear to follow approximately the same bi-modal form as in the case of $h = 0$.